Accepted Manuscript

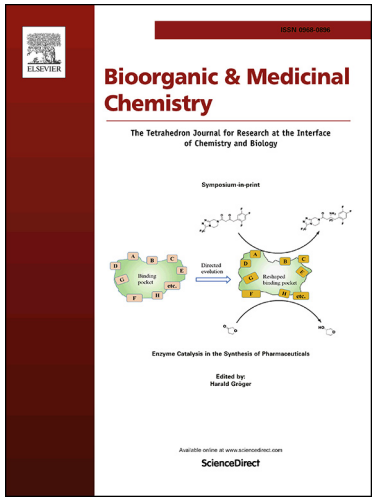

Dual-targeting for brain-specific liposomes drug delivery system: synthesis and preliminary evaluation

Yao Peng, Yi Zhao, Yang Chen, Zhongzhen Yang, Li Zhang, Wenjiao Xiao, Jincheng Yang, Li Guo, Yong Wu

PII: S0968-0896(18)30915-5
DOI: https://doi.org/10.1016/j.bmc.2018.08.006
Reference: BMC 14493

To appear in: *Bioorganic & Medicinal Chemistry*

Received Date: 12 May 2018
Revised Date: 25 July 2018
Accepted Date: 4 August 2018

Please cite this article as: Peng, Y., Zhao, Y., Chen, Y., Yang, Z., Zhang, L., Xiao, W., Yang, J., Guo, L., Wu, Y., Dual-targeting for brain-specific liposomes drug delivery system: synthesis and preliminary evaluation, *Bioorganic & Medicinal Chemistry* (2018), doi: https://doi.org/10.1016/j.bmc.2018.08.006

Dual-targeting for brain-specific liposomes drug delivery system: synthesis and preliminary evaluation

Yao Peng[a], Yi Zhao[a], Yang Chen[a], Zhongzhen Yang[a], Li Zhang[a], Wenjiao Xiao[a], Jincheng Yang[b], Li Guo[a]*, Yong Wu[a]*

[a]*Key Laboratory of Drug Targeting and Drug Delivery System of Education Ministry, Department of Medicinal Chemistry, West China School of Pharmacy, Sichuan University, Chengdu 610041, P. R. of China.*

[b]*Department of Pharmacy, National Cancer Center/Cancer Hospital, Chinese Academy of Medical Sciences and Peking Union Medical College, Beijing 100021, P. R. of China.*

Abstract: The treatment of glioma has become a great challenge because of the existence of brain barrier (BB). In order to develop an efficient brain targeting drug delivery system to greatly improve the brain permeability of anti-cancer drugs, a novel brain-targeted glucose-vitamin C (Glu-Vc) derivative was designed and synthesized as liposome ligand for preparing liposome to effectively deliver paclitaxel (PTX). The liposome was prepared and its particle size, zeta potential, encapsulation efficiency, release profile, stability, hemolysis and cytotoxicity were also characterized. What's more, the cellular uptake of CFPE-labeled Glu-Vc-Lip on $GLUT_1$- and $SVCT_2$-overexpressed C6 cells was 4.79-, 1.95-, 4.00- and 1.53-fold higher than that of Lip, Glu-Lip, Vc-Lip and Glu+Vc-Lip. Also, the Glu-Vc modified liposomes showed superior targeting ability *in vivo* evaluation compared with naked paclitaxel, non-coated, singly-modified and co-modified by physical blending liposomes. The relative uptake efficiency was

* Correspondence authors. Tel +86 28 85503777 (L. Guo), +86 28 85503235 (Y. Wu).
E-mail addresses: guoli@scu.edu.cn (L. Guo), wyong@scu.edu.cn (Y. Wu).

enhanced by 7.53 fold to that of naked paclitaxel, while the concentration efficiency was up to 7.89 times. What's more, the Glu-Vc modified liposomes also displayed the maximum accumulation of DiD-loaded liposomes at tumor sites with the strongest fluorescence in the brain *in vivo* imaging. Our results suggest that chemical modification of liposomes with warheads of glucose and vitamin C represents a promising and efficient strategy for the development of brain-specific liposomes drug delivery system by utilizing the endogenous transportation mechanism of the warheads.

Keywords: glucose, ascorbic acid, drug delivery, dual-targeting, liposomes, brain barrier

1. Introduction

With the rapid development of medical science, many diseases have been conquered over the past few decades. While, the central nervous system (CNS) diseases, such as brain tumor, have become one of the most dangerous threats to human health,[1,2] due to dramatic increase of brain diseases and their lower recovery. So, the treatment of brain tumor needs to be solved urgently. However, the two physiological barriers that separate the brain from its blood supply, would significantly decrease the accumulation of anti-cancer drug (including paclitaxel) in the brain and lead to an extremely limited distribution in CNS.[3]

One is the blood-brain barrier (BBB) and the other is the blood-cerebrospinal fluid barrier (BCSFB).[4-10] The barriers control the entry and exit of endogenous and exogenous compounds. Generally, the capability of molecules to cross the barriers by passive diffusion is related to their molecular weight, lipid solubility, charge, hydrogen bonding, ionization profile and physicochemical characteristics.[11,12] As a result, over 98% of small molecule drugs and all the macromolecular drugs could not reach the therapeutic concentration in the brain. Although the vascular-corrected brain concentration could be enhanced by increasing the dose of drug in treatments, it could cause serious side effects and severer toxicity meanwhile.

Therefore, there is a huge amount of demand of, not only for paclitaxel (PTX) but in general, strategies that can effectively deliver drugs into the brain for the treatment of brain tumor. [13-15]

Because of the high transport affinity between the transporter and substance, carrier-mediated transporter (CMT) system has become one of the most promising methods to facilitate the delivery of drugs into brain.[16,17] There are plenty of physiological transport systems for nutrients and endogenous compounds, for example, glucose transporter 1 ($GLUT_1$), sodium-dependent vitamin C transporter 2 ($SVCT_2$), large neutral amino acid transporter 1 (LAT_1) and monocarboxylic acid transporter 1 (MCT_1).[18-20]

$GLUT_1$ and $SVCT_2$ over-expressed on the surface of brain capillary endothelial cells and choroid plexus epithelium cells respectively, are considered as the most efficient transportation systems.[7,12]

It is well known that the enormous and sustained energy demand of the brain is provided almost exclusively by $GLUT_1$-transported glucose (Glu). It is estimated that transport value of $GLUT_1$ is 15-3000 fold more than other transporters. Liposomes modified by glucose have been proposed as a strategy to improve their brain uptake. Moreover, it has been widely reported that C-6 position glycosylation is an effective way to heighten the accumulation of drugs in brain.[22,23] Our previous studies have also shown that the liposomes modified with glucose could be transported into brain specifically and subsequently release the drugs, hence increasing the concentration in the brain.[16,19] These evidences all suggested that glucose could be used as a good carrier for brain targeting drugs.

In addition to glucose, it was also widely reported that the vitamin C (Vc) derivatives have a superior brain targeting efficiency. Studies have indicated that there is a highest concentration of Vc in the brain, which is 10 fold more than that in other organs.[24] In general, Vc is transported into the brain mainly through two different ways. One is the sugar transporter $GLUT_1$, which can transport dehydro-vitamin C

(DHVC, the oxidized form of Vc and can be reduced to Vc in brain). The other way is the transporter $SVCT_2$ which transports Vc into cerebrospinal fluid (CSF) at the choroid plexus, from which Vc can be further diffused to brain extracellular fluid (ECF), and then taken up into the brain cells from ECF. What's more, it was reported that the hydroxyl groups of enediol lactone in C2 and C3 are vital reaction sites for Vc in the redox process, while the C5- and C6-hydroxyl groups of Vc are not critical for its transportation.[25] Therefore, the modification of Vc is always conducted at C5 and C6 sites. Given all the evidences, it is also a promising method to utilize Vc and its transporters to improve the brain targeting ability.

Recently, some studies have explored the possibility of using Glu or Vc as carriers to promote the permeation across the BB into brain. But single-modification with Glu or Vc has limited targeting efficiency with 2-4 fold increase.[16,18,19] In our previous work, we designed and synthesized dual-brain targeting ibuprofen prodrugs, which had much better efficiency *in vitro* and *in vivo* than the parent drug and the single-modified prodrugs.[11] In this study, we will explore the possibility to develop a brain-targeting liposomes drug delivery system which uses glucose and vitamin C as the mediators to improve the brain permeability. We aim to construct a dual-targeting moiety Glu-Vc-Chol as liposomes ligand to delivery PTX into brain effectively. What's more, the Glu-Vc modified, non-coated, singly-modified and co-modified by physical blending liposomes (Glu+Vc-Lip) were prepared by the lipid film hydration-ultrasound method, and the characteristics and brain target abilities were conducted *in vitro* and *in vivo*.

2. Results and discussion

2.1. Synthesis of liposomes ligands

The synthetic route of ligand Glu-Vc-Chol was illustrated in Scheme 1. Firstly, we synthesized the glycosylated derivative **5** and the ascorbic acid intermediate **9**. Briefly, glucose **1** was totally etherified with chlorotrimethylsilane (TMSCl) and hexamethyl disilazane in pyridine to give penta-O-trimethylsilyl-glucopyranose **2**, which was treated by the mixture of acetone, acetic acid and methanol to deprotect the C-6 TMS group selectively to obtain compound **3**. Then, the linker 4-(benzyloxy)-4-oxobutanoic acid was connected with intermediate **3** to generate compound **4**. After deprotecting the benzyl group from **4**, glucose-TMS derivative **5** was obtained.[12] The synthesis of intermediate **9** started from the available material Vc. Treatment of **6** with acetyl chloride in acetone following our earlier method afforded 5,6-O,O-isopropylidene protected Vc ketol **7**. Benzylation of the C-2 and C-3 hydroxy groups of the ketol **7** was accomplished using K_2CO_3 and benzyl bromide in acetone to provide **8**. Deblocking of the 5,6-O,O-protected derivative of **8** with HCl in CH_3CN solution gave 2,3-O,O-dibenzyl Vc intermediate **9**.[7] What's more, cholesterol **10** underwent five steps to generate compound **15**,[13] which was then conjugated with glycosylated derivative **5** in the presence of DCC and DMAP to give compound **16**. Finally, compound **16** was readily underwent a deprotection reaction to get compound **17** when subjected the condition of trifluoroacetic acid in dichloromethane, then the 2,3-O-di-benzyl groups of **17** was removed under hydrogen catalyzed by Pd/C to provide the target ligand Glu-Vc-Chol.

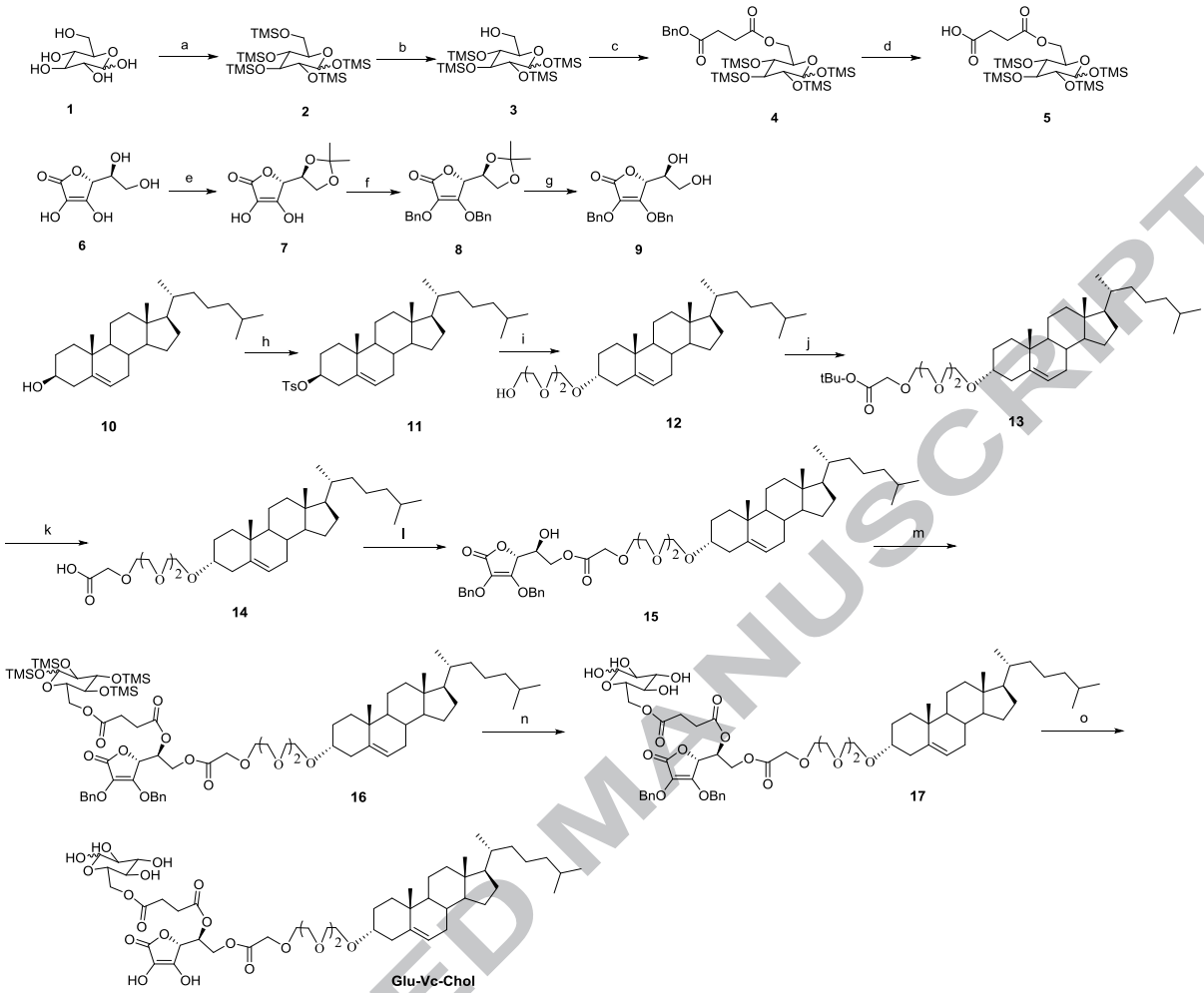

Scheme 1. Synthesis of ligand Glu-Vc-Chol. Reagents and conditions: (a) HMDS, TMSCl, pyridine, 0 °C - r.t.; (b) AcOH, CH_3OH, acetone, 0 °C; (c) 4-(benzyloxy)-4-oxobutanoic acid, DCC, DMAP, CH_2Cl_2, r.t.; (d) Pd/C, H_2, methanol, r.t.; (e) acetone, AcCl, r.t., 24 h; (f) K_2CO_3, BnBr, acetone, reflux, 5 h; (g) HCl, CH_3CN, r.t., 3 h; (h) TsCl, pyridine, 50°C, 5 h; (i) Triethylene glycol, dioxane, reflux, 6 h; (j) *t*-butyl bromoacetate, *n*-$Bu_4N^+HSO_4$, 50% NaOH, toluene, r.t., 16 h; (k) TsOH, tolunene, reflux 8 h; (l) **9**, DCC, DMAP, CH_2Cl_2, r.t., 4 h; (m) **5**, DCC, DMAP, CH_2Cl_2, r.t., 5 h; (n) TFA, CH_2Cl_2, r.t., 1 h; (o) Pd/C (10%), H_2, CH_3OH, 1 h.

The synthetic route of ligand Vc-Chol was illustrated in Scheme 2. Briefly, the 2,3-O-di-benzyl groups of **15** was removed under hydrogen catalyzed by Pd/C to provide the target ligand Vc-Chol. All the title compounds and important intermediates were characterized by their respective ^1H NMR and MS.

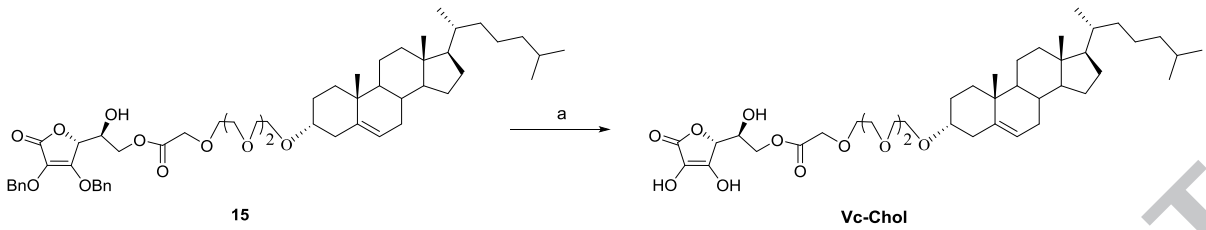

Scheme 2. Synthesis of ligand Vc-Chol. Reagents and conditions: (a) Pd/C (10%), H_2, CH_3OH, 1 h.

2.2. Preparation and characterization of liposomes

One of the requirement for liposomes to penetrate BBB is that they must have proper sizes and uniform distribution. The particle sizes and zeta potentials of different liposomes in this study were listed in Table 1. The encapsulation efficiencies (EE%) of paclitaxel in the each type of liposomes were all greater than 82%. The average particle sizes of all liposomes were less than 110 nm, and the values of polymer dispersity index (PDI) were close to 0.19. What's more, the transmission electron microscopy (TEM) of PTX-Glu-Vc-Lip showed that the liposomes exhibited uniform spherical in shape (Fig. 1). To our knowledge, the particle size and zeta potential of liposomes were crucial to *in vivo* study.[20]

Table 1 Particle sizes and zeta potentials of different liposomes and the PTX entrapment efficiency of PTX-loaded liposomes (n =3, mean ± SD).

	Size (nm)	PDI	Zeta potential (mV)	EE (%)
PTX-Lip	105.8 ± 2.5	0.188 ± 0.023	-2.08 ± 0.12	90.57 ± 3.84
PTX-Glu-Lip	106.3 ± 1.4	0.193 ± 0.009	-3.45 ± 0.29	88.54 ± 5.01
PTX-Vc-Lip	102.9 ± 1.7	0.198 ± 0.017	-2.88 ± 0.33	89.62 ± 2.97
PTX-Glu-Vc-Lip	109.2 ± 3.3	0.185 ± 0.025	-4.13 ± 0.20	86.37 ± 4.68
PTX-Glu+Vc-Lip	108.5 ± 2.6	0.186 ± 0.014	-4.66 ± 0.45	87.51 ± 6.17

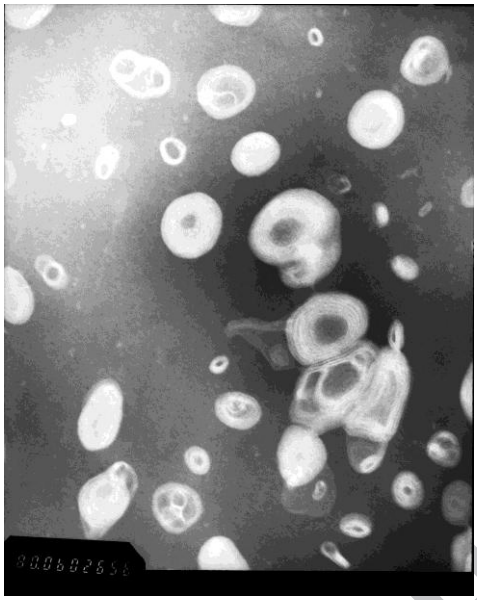

Fig. 1. The TEM image of PTX-Glu-Vc-Lip

2.3. In vitro drug release study

PTX release properties were evaluated in PBS containing 0.1% Tween 80. As shown in Fig. 2, for free PTX, the release exhibited a rapid property, with over 80% of the drug released into the media within 12 h incubation. On the other hand, the PTX-loaded liposomes exhibited the sustained release behaviors, with the cumulative PTX released from liposomes was less than 60% after 48 h incubation. No significant difference on release properties was observed among PTX-Lip, PTX-Glu-Lip, PTX-Vc-Lip, PTX-Glu-Vc-Lip and PTX-Glu+Vc-Lip, and none of these PTX-loaded liposomes displayed burst initial release patterns.

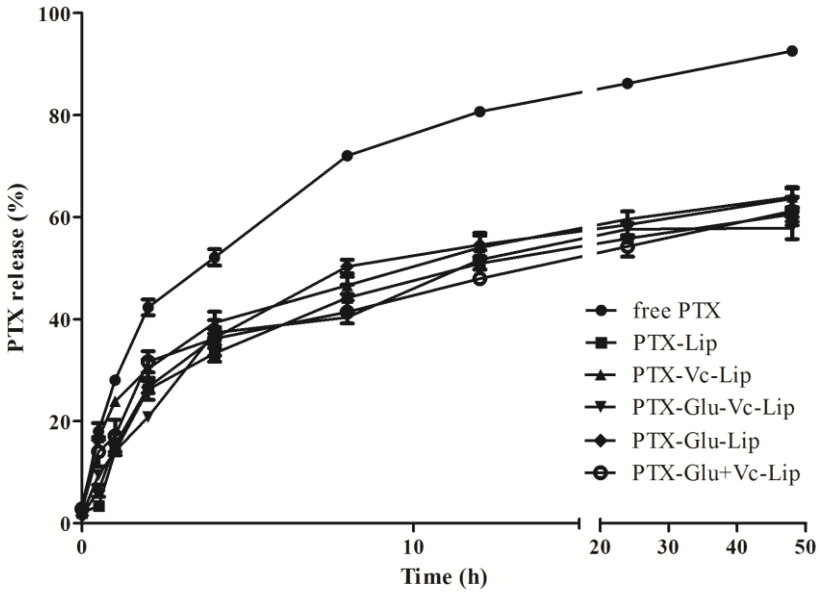

Fig.2. The PTX release profiles of free PTX, PTX-Lip, PTX-Glu-Lip, PTX-Vc-Lip, PTX-Glu-Vc-Lip and PTX-Glu+Vc-Lip in PBS (pH 7.4) containing 0.1% Tween 80 over 48 h (n = 3, mean ± SD).

2.4. In vitro stability of liposomes in serum

It is important for liposomes to have superior stability in biological conditions, which is closely related to governing the activity of the associated therapeutic agent. Transmittance of different liposomes were monitored in the presence of 50% FBS. As shown in Fig. 3, the transmittance of the liposomes were above 90% and hardly changed after 48 h incubation with 50% FBS. This stability study of liposomes indicated that the liposomes were able to prevent the interaction between liposomes and serum protein, which was important for the long blood half-life *in vivo*.

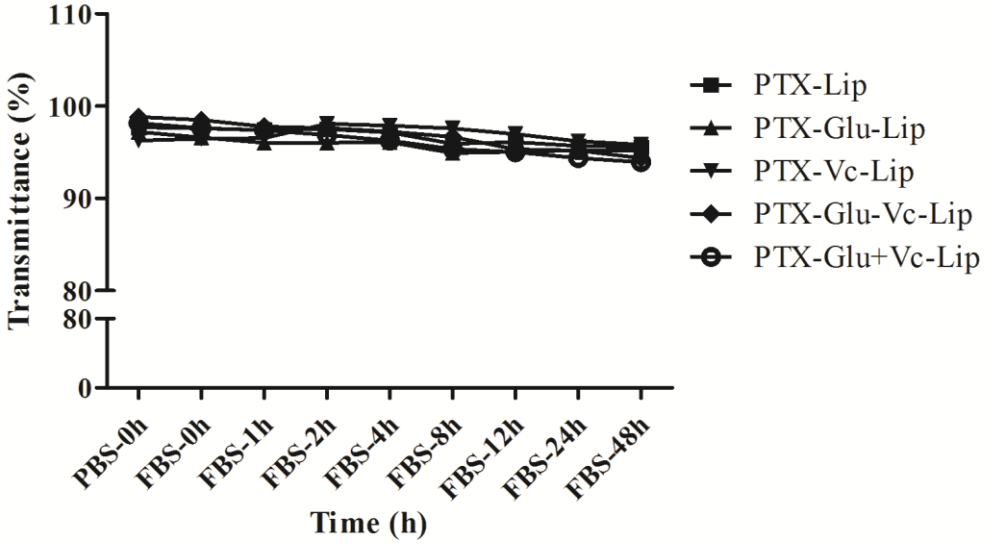

Fig. 3. Serum stability (represented by transmittance) of Lip, Glu-Lip, Vc-Lip, Glu-Vc-Lip and Glu+Vc-Lip in 50% FBS over 48 h (n = 3, mean ± SD).

2.5.Hemolysis assays

Hemocompatibility is a key point for in vivo applications of liposomes. As shown in Fig. 4, hemolysis assay of ligand-modified liposomes demonstrated that all the liposomes did not significantly increase the hemocompatibility (less than 10%) even the concentration of phospholipids up to 400 nmoles, which indicated that the lipid material was almost no-toxic..

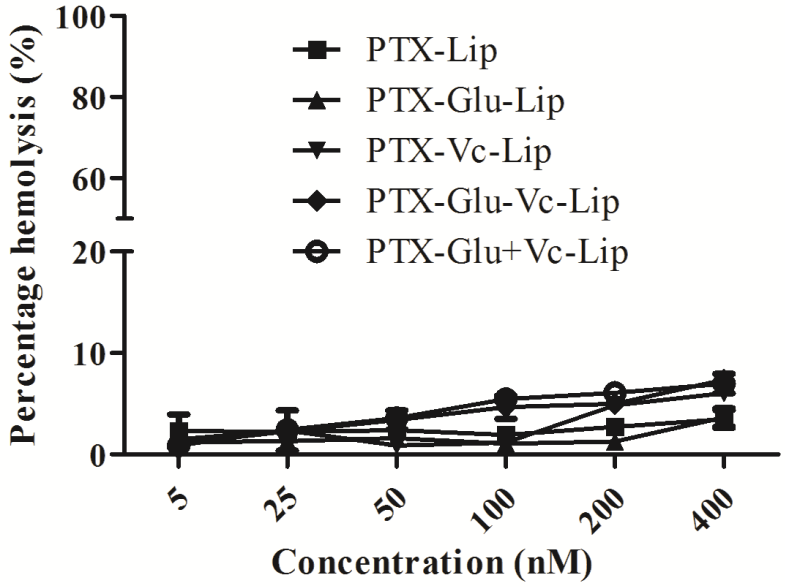

Fig. 4. Hemolysis percentage of various concentrations of Lip, Glu-Lip, Vc-Lip, Glu-Vc-Lip and Glu+Vc-Lip after incubation for 1 h at 37 °C (n = 3, mean ± SD).

2.6.Cytotoxicity

The cytotoxicity of different liposomes on C6 cells was evaluated using MTT assay. As shown in Fig. 5A, free PTX showed higher inhibition rate than PTX-loaded liposomes, which may be because that free drugs could be transported into the cells directly by passive diffusion, without a drug release process. What's more, among the five groups of liposomes, PTX-Glu-Vc-Lip had the lowest cell viability, which may due to the transport by the two transporters. On the other hand, the cytotoxicity of blank liposomes was also measured, and all these five kinds of blank liposomes exhibited no significant cytotoxicity (Fig. 5B). Therefore our liposomal drug delivery systems were safe and nontoxic to be further used *in vivo*.

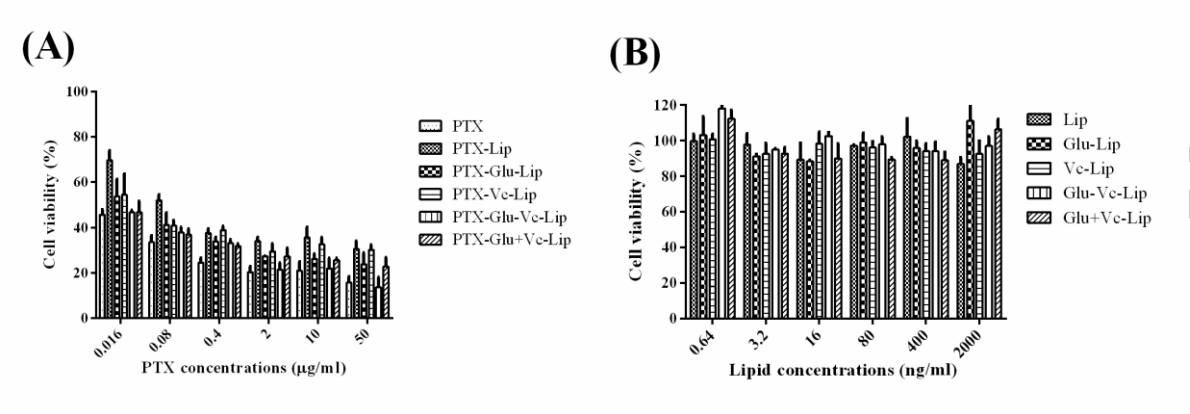

Fig. 5. (A) The cytotoxicity study on C6 cells after treated with various concentrations of PTX-Lip, PTX-Glu-Lip, PTX-Vc-Lip, PTX-Glu-Vc-Lip and free PTX for 24 h (n = 3, mean ± SD). (B) The cytotoxicity study on C6 cells after treated with various concentrations of Lip, Glu-Lip, Vc-Lip, Glu-Vc-Lip and Glu+Vc-Lip for 24 h (n = 3, mean ± SD).

2.7.Cellular uptake

To access whether Glu-Vc-Lip could deliver more drugs into cells than other groups of liposomes, the $GLUT_1$ and $SVCT_2$-positive C6 cells were chosen as the cell model. It could be seen from Fig. 6A that the uptake of ligand-modified liposomes was significantly higher compared with the conventional liposomes (Lip). What's more, the uptake of Glu-Vc-Lip showed 4.79, 1.95, 4.00 and 1.53 time higher than that of Lip, Glu-Lip, Vc-Lip and Glu+Vc-Lip, respectively, which indicated that the Glu-Vc moiety exhibited better penetrability in C6 glioma cells.

The images by confocal laser scanning microscope (CLSM) (Fig. 6B) were well consistent with the above results by a flow cytometer. The green fluorescence can be clearly observed in Glu-Vc-Lip, which was much stronger than that of other groups. All the results showed that Glu-Vc-Lip had better targeting property to $GLUT_1$- and $SVCT_2$-expressed C6 cells.

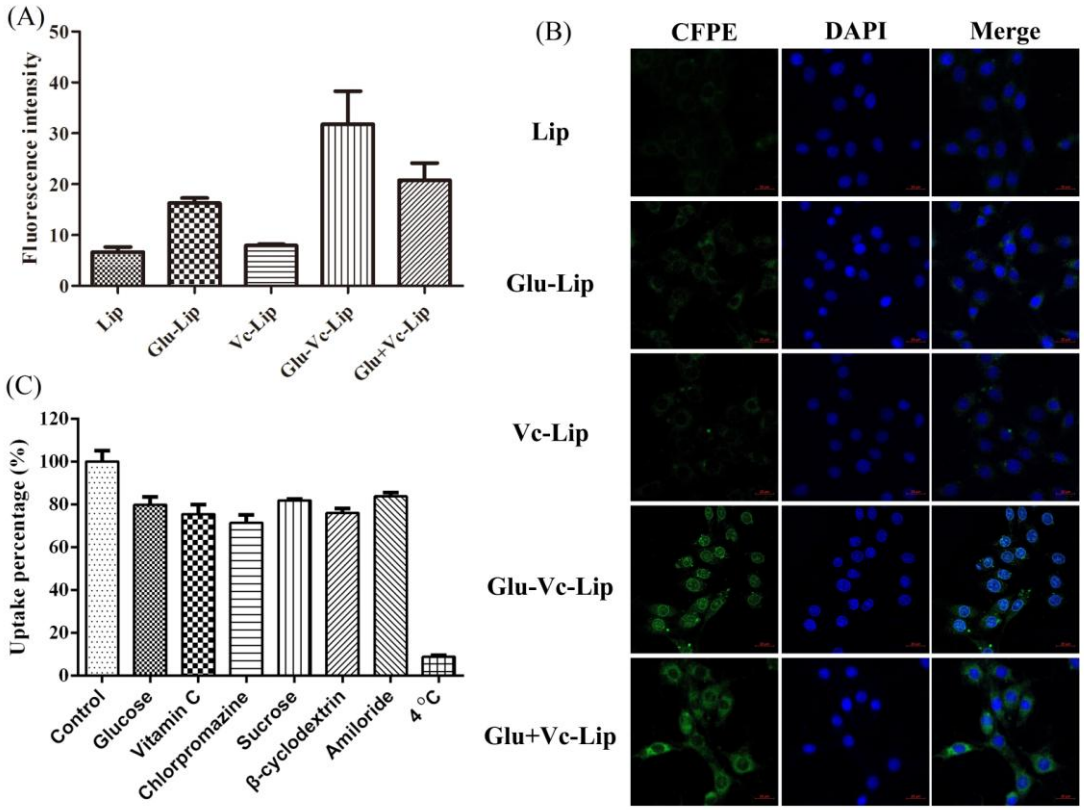

Fig. 6. Cellular uptake of CFPE-labeled Lip, Glu-Lip, Vc-Lip, Glu-Vc-Lip and Glu+Vc-Lip on C6 cells. (A) Quantitative 4 h cellular uptake of CFPE-labeled liposomes determined by flow cytometer (mean ± SD, n = 3). (B) Qualitative 4 h cellular uptake of CFPE-labeled liposomes determined by CLSM, green (CFPE-labeled liposomes), blue (DAPI stained nucleus), light blue (colocalized CFPE and DAPI). Scale bars represent 10 μm. (C) The relative uptake of CFPE-labeled Glu-Vc-Lip on C6 cells for 4 h after preincubation of different endocytosis inhibitors determined by flow cytometer (mean ± SD, n = 3).

In order to further study the penetrability of Glu-Vc-Lip, the uptake mechanism was conducted by using a series of endocytosis inhibitors to pre-incubate with C6 cells, and then calculating the inhibition rate. As shown in Fig. 6C, the preincubation of free glucose or free Vc could competitively inhibited the uptake of Glu-Vc-Lip on C6 cells. This further proved that the glucose domain and Vc domain of liposomes increased the cellular internalization by specifically binding to $GLUT_1$ and $SVCT_2$. Furthermore, the effects of clathrin-mediated endocytosis on the internalization of the Glu-Vc-Lip were evaluated using chlorpromazine and sucrose, a kind of clathrin-coated pits formation blocking agent. β-cyclodextrin, agent

disrupting caveolae, was used to evaluate the effect of caveolae-mediated endocytosis on the internalization of the Glu-Vc-Lip. Amiloride was chosen to block micropinocytosis. As the results showed, every inhibitor showed different levels of inhibition effects. 4 ^{o}C also had a strong effect on cellular uptake (down to 8.70%), suggesting energy-dependent properties of endocytosis. All the results indicated that Glu-Vc-Lip could be recognized by glucose transporter $GLUT_1$ and $SVCT_2$ on the outer membrane of cells via the residues on the surface, and then energy-dependently internalized through a synthetic endocytic pathway including clathrin-mediated, caveolae-mediated and micropinocytosis-mediated endocytosis.

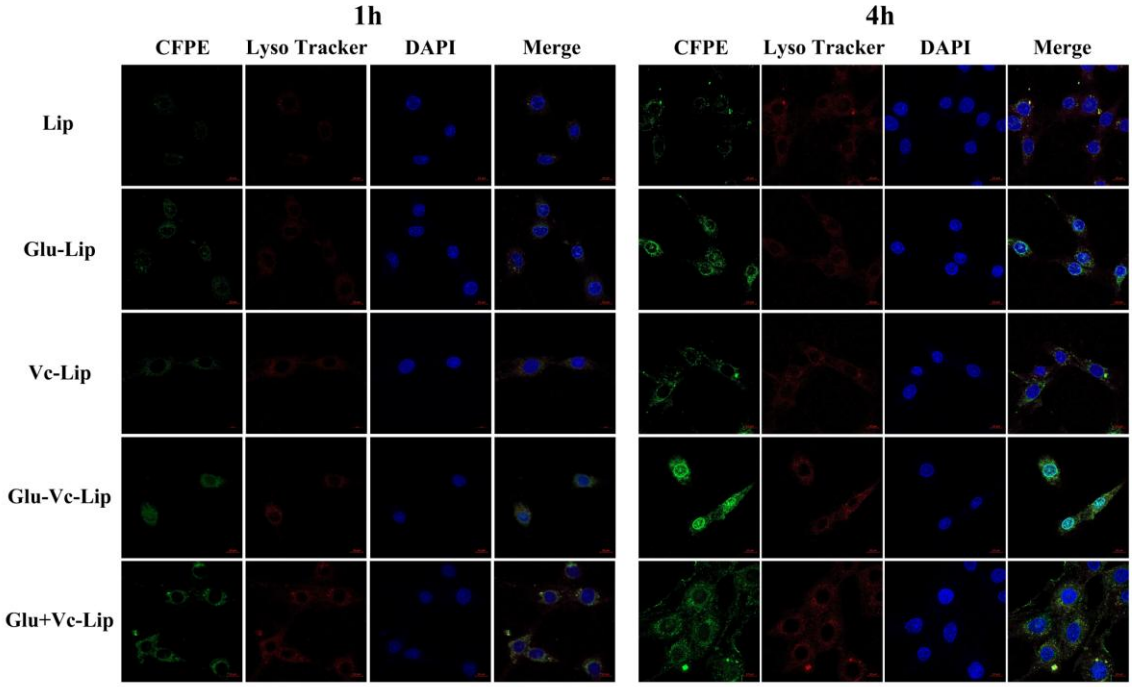

Fig. 7. Intracellular localization of Lip, Glu-Lip, Vc-Lip, Glu-Vc-Lip and Glu+Vc-Lip on C6 cells determined by CLSM, green (CFPE-labeled liposomes), blue (DAPI stained nucleus), red (LysoTracker stained lysosome), light blue (colocalized CFPE and DAPI), yellow (colocalized CFPE and Lyso Tracker). Scale bars represent 10 μm.

To elucidate the intracellular localization of liposomes after uptake, the lysosomes were labeled with Lyso-Tracker RED and the nucleus were dyed with DAPI, which were imaged by CLSM. Lysosomes were visualized as the RED fluorescence, while CFPE-labeled liposomes were shown as the green fluorescence.

Co-localization of liposomes with the lysosomes was indicated by yellow. As the Fig. 7 showed, after 1h incubation, it was similar in each group that most of the liposomes taken up by the cells were found to localize in the lysosome of C6 cells. With the incubation time increasing, the green fluorescence intensity was much higher than that of 1 h, suggesting that the cellular uptake of the liposomes exhibited a time-dependent pattern. What's more, the increased co-localization of Glu-Vc-Lip was poorer after 4h incubation than other groups, which might be due to a large proportion of the Glu-Vc-lip entered into the nucleus as the nucleus dyed with DAPI showing a co-localization with the green fluorescence of CFPE. All the results indicated that the internalization of Glu-Vc-Lip was mediated by lysosomes and a part of it could escape from lysosomes, which may be because endosomes are the main organelles that internalize foreign materials and particles and the abundance of Glu-Vc-Lip taken up into cells increased its chances of entering the nucleus.

2.8 Distribution Study in Plasma and Brain

For *in vivo* study, PTX-Lip, PTX-Glu-Lip, PTX-Vc-Lip, PTX-Glu-Vc-Lip, PTX-Glu+Vc-Lip and paclitaxel original drug were injected through the tail vein with the dose of 10 mg/kg body weight of paclitaxel. At 5, 15, 30, 60, 120, 240, 480 and 1440 min after injection, blood and brain were collected to analyze the concentration of paclitaxel by HPLC method.

The plasma PTX concentration-time profiles were shown in Fig. 8 and the pharmacokinetic parameters of PTX from different formulations were summarized in Table 2. The results showed that the liposomes could significantly enhance the concentration-time profile (AUC_{0-t}) of paclitaxel compared with the naked paclitaxel within 24 h. The AUC_{0-t} of PTX-Glu-Vc-Lip was increased by about 1.58-time than that of free PTX. It was also shown that PTX-Glu-Vc-Lip could extend the elimination half-life ($t_{1/2}$) of free PTX from 218 min to 501 min. These data indicated that the liposomes possessed certain stability in plasma, with

more chance to be transported into brain.

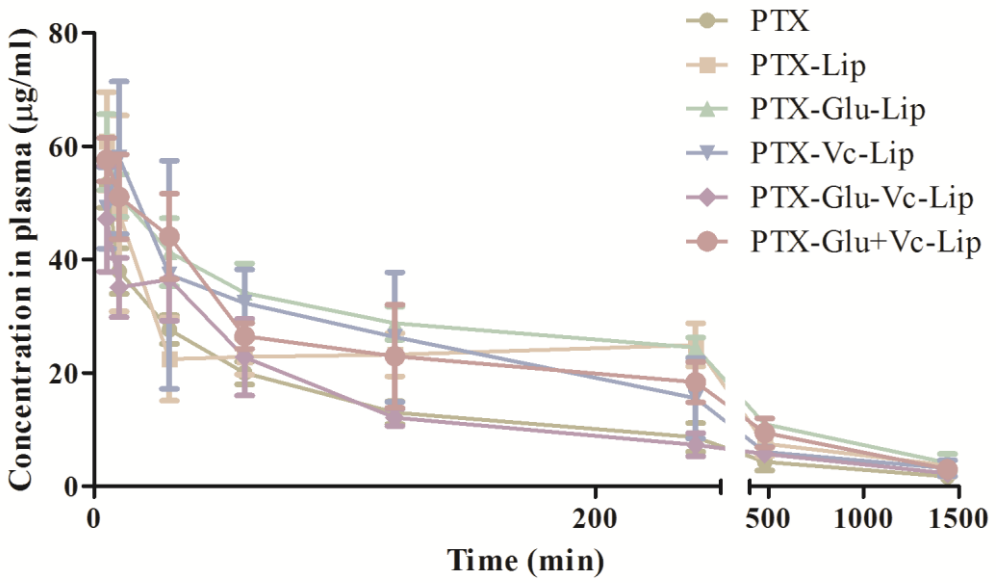

Fig. 8. The concentration curve of paclitaxel versus time in plasma after i.v. injection of PTX-Lip, PTX-Glu-Lip, PTX-Vc-Lip, PTX-Glu-Vc-Lip, PTX-Glu+Vc-Lip and PTX in mice with the dose of 10 mg/kg (mean ± SD, n = 3).

Table 2. Pharmacokinetic parameters of paclitaxel in blood after administration of paclitaxel and liposomes (n=3)

	Paclitaxel	PTX-Lip	PTX-Glu-Lip	PTX-Vc-Lip	PTX-Glu-Vc-Lip	PTX-Glu+Vc-Lip
$AUC_{(0-t)}$ (μg/g·min)	8630.66 ± 1591.81	15557.77 ± 2386.18	19509.51 ± 1590.99	13856.47 ± 1266.75	13647.47 ± 336.26	15872.73 ± 867.93
MRT (min)	351.77 ± 41.81	390.41 ± 64.74	386.35 ± 34.68	360.81 ± 64.93	389.11 ± 2.10	375.31 ± 29.02
T_{max} (min)	5	6.66	5	8.33	5	6.66
C_{max} (μg/g)	53.33 ± 4.16	65.42 ± 5.76	56.44 ± 5.91	58.92 ± 13.19	47.21 ± 9.34	58.08 ± 4.02
$t_{1/2}$ (min)	218.31 ± 50.88	391.75 ± 243.82	478.86 ± 113.42	403.77 ± 65.02	501.41 ± 197.66	364.42 ± 98.34

$AUC_{(0-t)}$: the area under the curve from 0 h to t h. MRT: the mean residence time. T_{max}: the time to maximum concentration. C_{max}: the maximum concentration. $t_{1/2}$: the elimination half-life.

To further evaluate the possibility of the Glu-Vc-mediated liposomes being transported across BBB, the distribution in brain of PTX-loaded liposomes and paclitaxel was determined. The concentrations of

paclitaxel in brain versus time curves were displayed in Figure 9 and the pharmacokinetic parameters were listed in Table 3.

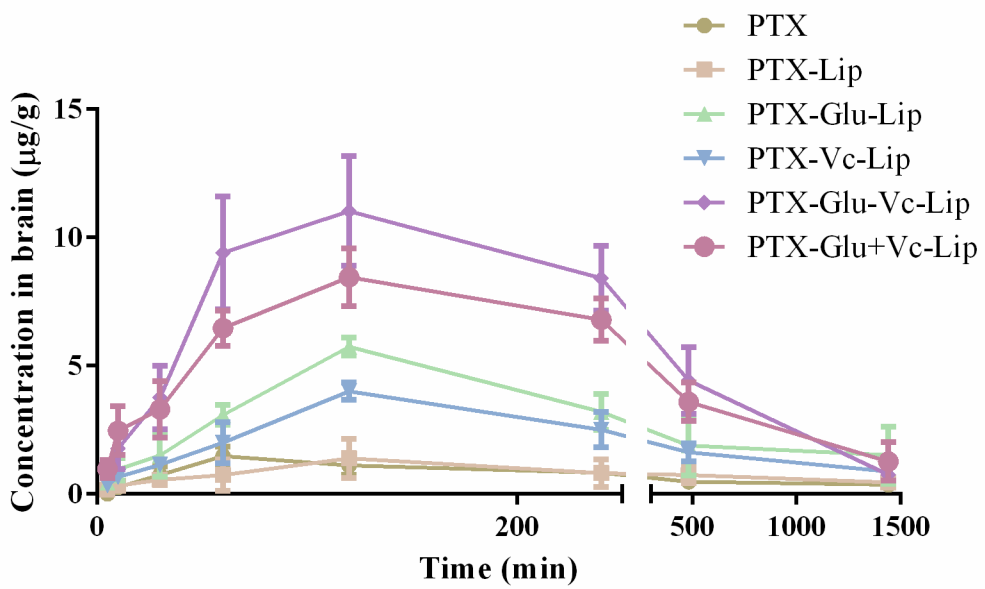

Fig. 9. The concentration curve of paclitaxel versus time in brain after i.v. injection of PTX-Lip, PTX-Glu-Lip, PTX-Vc-Lip, PTX-Glu-Vc-Lip, PTX-Glu+Vc-Lip and PTX in mice with the dose of 10 mg/kg. (mean ± SD, n = 3).

Table 3. Pharmacokinetic parameters of paclitaxel in brain after administration of paclitaxel and liposomes (n=3)

	Paclitaxel	PTX-Lip	PTX-Glu-Lip	PTX-Vc-Lip	PTX-Glu-Vc-Lip	PTX-Glu+Vc-Lip
$AUC_{(0-t)}$ (μg/g·min)	807.22 ± 235.63	991.39 ± 239.77	3150.24 ± 1317.91	2341.21 ± 264.80	6075.76 ± 918.10	5164.32 ± 1071.04
MRT (min)	547.68 ± 57.65	583.91 ± 113.41	542.39 ± 107.44	523.79 ± 41.51	381.14 ± 10.70	441.68 ± 55.97
T_{max} (min)	60	160	120	120	100	120
C_{max} (μg/g)	1.48 ± 0.37	1.60 ± 0.50	5.74 ± 0.35	4.00 ± 0.34	11.68 ± 1.96	8.45 ± 1.12
$t_{1/2}$ (min)	339.52 ± 187.65	576.21 ± 191.59	670.81 ± 141.43	942.33 ± 513.48	351.36 ± 56.27	373.26 ± 69.77
Re	-	1.23	3.90	2.90	7.53	6.40
Ce	-	1.08	3.90	2.70	7.89	5.71

Re: the relative uptake efficiency. Ce: the concentration efficiency.

In brain, it is obvious that all of the liposomes could be delivered to the brain through i.v. administration.

At all the predetermined time points, the concentration of paclitaxel released from liposomes was much higher than that from paclitaxel original drug during 24 h. The AUC_{0-t} and C_{max} of paclitaxel from liposomes were fairly higher than that of free paclitaxel. The relative uptake efficiencies (Res) of PTX-Lip, PTX-Glu-Lip, PTX-Vc-Lip, PTX-Glu-Vc-Lip and PTX-Glu+Vc-Lip were enhanced to 1.23, 3.90, 2.90, 7.53 and 6.40 times than that of naked paclitaxel, respectively. The concentration efficiencies (Ces) were also enhanced to 1.08, 3.90, 2.70, 7.89 and 5.71 times than that of paclitaxel. So these data further proved our conjecture that liposome with dual-targeting ligand Glu-Vc-Chol had superior brain-targeting efficiency.

2.9 In vivo imaging

Kunming mice bearing C6 glioma were used to estimate the glioma targeting efficiency of different liposomes. Fig. 10A showed the *in vivo* images of intracranial C6 glioma bearing mice at 1, 2, 6, 24 h after systemic administration of DiD-loaded liposomes. And then the mice were sacrificed at pre-determined time points, and the brains, hearts, livers, spleens, lungs and kidneys were harvested and imaged. *Ex vivo* images of the brains were exhibited in Fig. 10C and other organs were shown in Fig. 10B. The strongest fluorescence signal of the all the liposomes in the brain was obviously observed 2 h after injection, which was consistent with the result of the distribution study. The co-modified liposomes Glu-Vc-Lip exhibited the best ability to accumulate at the tumors with much stronger fluorescence than singly-modified and non-modified liposomes and even a little stronger than Glu+Vc-Lip in the brains. However, at 2 h and 6 h after injection, the strong fluorescence signal of different liposomes was also found in the livers and in part of the spleen, but no obvious signal was observed in heart, lung, and kidney, which may be due to the metabolism. These *in vivo* imaging results suggested that Glu-Vc on the surface of liposomes endowed the liposomes with brain glioma dual-targeted delivery capability. These findings were well consistent with

the results of *in vitro* cellular uptake study.

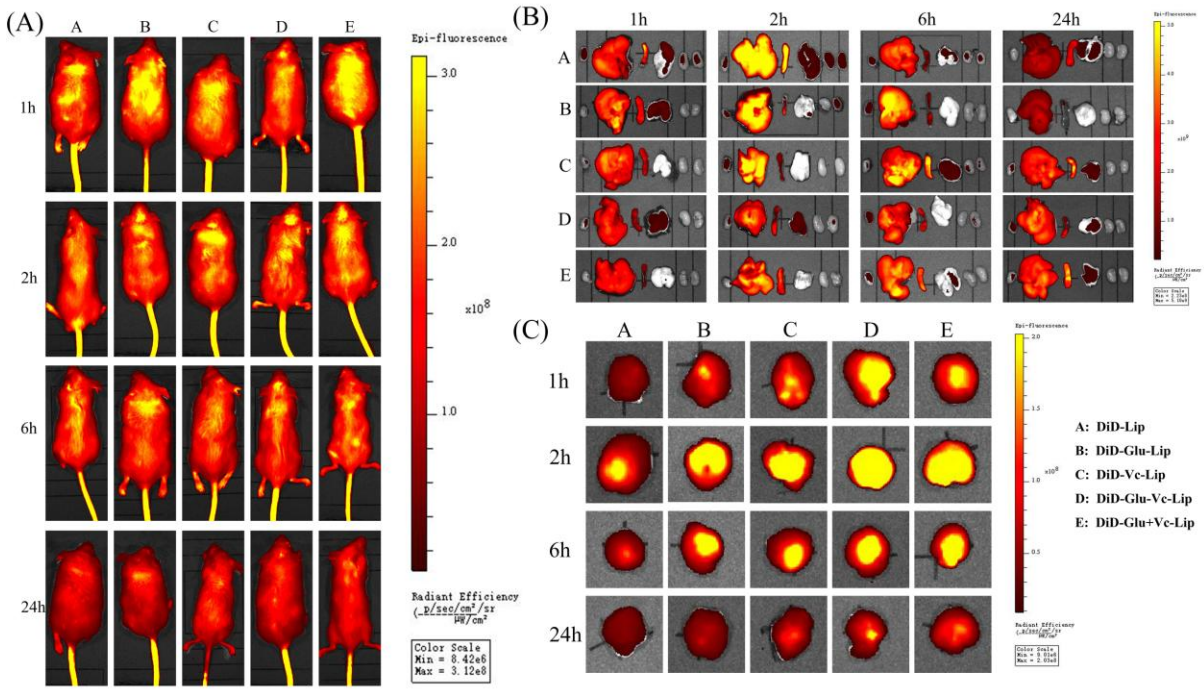

Fig. 10. (A) *In vivo* images of intracranial C6 glioma bearing mice at 1, 2, 6, 24h after systemic administration of Did-loaded liposomes. (B) *Ex vivo* images of the brains. (C) *Ex vivo* images of isolated organs and they were heart, liver, spleen, lung and kidney from left to right. A: DiD-Lip, B: DiD-Glu-Lip, C: DiD-Vc-Lip, D: DiD-Glu-Vc-Lip, E: DiD-Glu+Vc-Lip. (n=3)

3. Conclusion

In order to develop an efficient brain targeting drug delivery system to greatly improve the brain permeability of drugs, a novel dual-targeting glucose-Vc derivative was designed and synthesized as liposome ligand in this work. Glu-Vc-Lip could be recognized by glucose transporter $GLUT_1$ and $SVCT_2$ on the outer membrane of cells via the residues on the surface, and then energy-dependently internalized through a synthetic endocytic pathway including clathrin-mediated, caveolae-mediated and micropinocytosis-mediated endocytosis. What's more, Glu-Vc-Lip significantly increased the brain uptake of PTX *in vivo* with the increased Re and Ce, and the *in vivo* imaging of DiD-Glu-Vc -Lip showed significantly more fluorescent than other groups, suggesting that both glucose and vitamin C transporters

($GLUT_1$ and $SVCT_2$) might be involved to help the liposomes to penetrate the BB. Therefore, the Glu-Vc modification represents a promising strategy for the development of future brain-specific drug delivery systems.

4. Experimental section

4.1. Materials

The melting point was measured on an YRT-3 melting point apparatus (Shantou Keyi instrument & Equipment Co. Ltd, Shantou, China). NMR spectra were taken on a Varian INOVA 400 MHz (Varian, Palo Alto, CA, USA) using $CDCl_3$ as solvent. Chemical shifts are expressed in δ (ppm), with tetramethylsilane (TMS) functioning as the internal reference, and coupling constants (J) were expressed in Hz. Mass spectra were recorded on an Agilent 1946B ESI-MS instrument (Agilent, Palo Alto, CA, USA). Reversed-phase chromatography performed on C18 chromatographic analysis was carried out using the HPLC system (Alltech, IL, USA) consisted of a RF-530 fluorescence detector (Shimadzu, Japan) and Allchorom plus data operator, respectively. A Diamonsil column (200 × 4.6 mm, 5 μm) was used.

Kunming mice rats (20-25 g) were provided by the Laboratory Animal Center of Sichuan University (Chengdu, China). All animal study procedures were approved by the Sichuan University Animal Ethical Experimentation Committee according to the requirements of the National Act on the use of experimental animals (China).

4.2. Chemistry

*4.2.1 Synthesis of compound **2-14***

The synthesis of compound **2-14** was reported in our previous work.[7,12,16]

*4.2.2 Synthesis of compound **15***

To a solution of compound **14** (1.62 g, 2.81 mmol) in CH_2Cl_2 (40 ml) was added DCC (0.87 g, 4.22 mmol) and DMAP (68 mg, 0.56 mmol), and the reaction was stirred at -5 ^oC for 30 min. Then compound **9** (0.83 g, 2.34 mmol) in CH_2Cl_2 (10 ml) was added promptly. After stirring for another 4 h at r.t., the mixture was filtered and the filtrate was concentrated. Then the residue was purified by chromatography to give **15** (1.78 g, 69.2%) as a yellow oil. ^1H NMR (400 MHz, $CDCl_3$, ppm) δ: 0.67 (s, 3H), 0.86 (d, 6H, J = 6.4 Hz), 0.91 (d, 3H, J = 6.6 Hz), 0.98 (s, 3H), 0.67-2.37 (remaining cholesterol protons), 3.14-3.19 (m, 1H), 3.61-3.74 (m, 12H), 4.07-4.10 (m, 1H), 4.19 (s, 2H), 4.26-4.30 (m, 1H), 4.37-4.41 (m, 1H), 4.66 (d, 1H, J = 2.0 Hz), 5.07-5.22 (m, 4H), 5.30-5.33 (m, 1H), 7.20-7.22 (m, 2H), 7.34-7.38 (m, 8H).

*4.2.3 Synthesis of compound **16***

To a solution of compound **5** (0.64 g, 1.12 mmol) in CH_2Cl_2 (20 ml) was added DCC (0.31 g, 1.50 mmol) and DMAP (18 mg, 0.15 mmol), and the reaction was stirred at -5 ^oC for 30 min. Then compound **15** (0.69 g, 0.75 mmol) in CH_2Cl_2 (10 ml) was added promptly. After stirring for another 5 h at r.t., the mixture was filtered and the filtrate was concentrated. Then the residue was purified by chromatography to give **16** (0.64 g, 57.9%) as a yellow oil. ^1H NMR (600 MHz, $CDCl_3$, ppm) δ: 0.12-0.14 (m, 36H), 0.67 (s, 3H), 0.87 (d, 6H, J = 11.4 Hz), 0.91 (d, 3H, J = 6.0 Hz), 0.98 (s, 3H), 0.67-2.37 (remaining cholesterol protons), 2.48-2.51 (m, 2H), 2.60-2.63 (m, 2H), 3.15-3.18 (m, 1H), 3.34-3.41 (m, 2H), 3.62-3.71 (m, 13H), 3.77 (t, 1H, J = 8.4 Hz), 3.87-3.90 (m, 1H), 4.13 (d, 2H, J = 4.8 Hz), 4.31-4.41 (m, 3H), 4.80 (d, 1H, J = 1.8 Hz), 4.99 (d, 1H, J = 3.0 Hz), 5.12-5.24 (m, 4H), 5.33-5.42 (m, 2H), 7.23-7.24 (m, 2H), 7.33-7.41 (m, 8H).

*4.2.4 Synthesis of compound **17***

To a solution of compound **16** (0.21 g, 0.14 mmol) in CH_2Cl_2 (10 ml) was added trifluoracetic acid (0.21

ml, 2.86 mmol) at 0 °C and then the reaction was stirred for 1 h at room temperature. The mixture was concentrated and the residue was purified by chromatography to give compound **17** (0.14 g, 83.3%) as a colorless oil. ^{1}H NMR (400 MHz, $CDCl_3$, ppm) δ: 0.67 (s, 3H), 0.86 (d, 6H, J = 5.2 Hz), 0.91 (d, 3H, J = 6.4 Hz), 0.98 (s, 3H), 0.85-2.44 (remaining cholesterol protons), 2.50-2.55 (m, 4H), 3.09 (br, 3H), 3.15-3.20 (m, 2H), 3.33-3.45 (m, 2H), 3.52-3.57 (m, 2H), 3.63-3.70 (m, 14 H), 3.79 (t, 1H, J = 9.2 Hz), 3.99 (br, 1H), 4.14 (s, 2H), 4.28-4.45 (m, 4H), 4.78 (d, 1H, J = 2.4 Hz), 5.07-5.18 (m, 4H), 5.26 (d, 1H, J = 3.2 Hz), 5.33 (d, 1H, J = 4.4 Hz), 5.40 (br, 1H), 7.21-7.23 (m, 2H), 7.33-7.38 (m, 8H).

4.2.5 Synthesis of ligand Glu-Vc-Chol

To a solution of compound **17** (0.10 g, 0.085 mmol) in methanol (10 ml), Pd/C (10 mg, 10%) was added. Then, the mixture was stirred in hydrogen atmosphere at room temperature for 1 h. Pd/C was filtered, and the filtrate was concentrated to give ligand Glu-Vc-Chol (81 mg, 95.6%) as a colorless oil. ^{1}H NMR (400 MHz, $CDCl_3$, ppm) δ: 0.67 (s, 3H), 0.86 (d, 6H, J = 6.4 Hz), 0.91 (d, 3H, J = 6.0 Hz), 0.98 (s, 3H), 0.78-2.44 (remaining cholesterol protons), 2.63 (br, 3H), 3.18 (s, 1H), 3.48-3.66 (s, 16H), 3.49-4.36 (m, 7H), 4.86-5.45 (m, 9H), 5.33 (s, 1H). ESI-MS calculated for $C_{51}H_{80}O_{19}K$ $[M+K]^+$ 1035.5, found 1034.9.

4.2.6 Synthesis of ligand Vc-Chol

To a solution of compound **15** (0.25 g, 0.27 mmol) in methanol (30 ml), Pd/C (30 mg, 10%) was added. Then, the mixture was stirred in hydrogen atmosphere at room temperature for 1 h. Pd/C was filtered, and the filtrate was concentrated to give ligand Vc-Chol (0.19 g, 94.4%) as a colorless oil. ^{1}H NMR (400 MHz, $CDCl_3$, ppm) δ: 0.63 (s, 3H), 0.78 (d, 6H, J = 6.3 Hz), 0.85 (d, 3H, J = 6.6 Hz), 0.94 (s, 3H), 0.63-2.63 (remaining cholesterol protons), 3.22 (m, 1H), 3.66-3.79 (m, 12H), 4.15 (m, 1H), 4.24 (s, 2H), 4.37 (m, 2H), 4.80 (m, 1H), 5.34 (m, 1H). ESI-MS calculated for $C_{41}H_{66}O_{11}Na$ $[M+Na]^+$ 757.5, found 757.6.

4.2.7 Synthesis of ligand Glu-Chol

The synthesis of ligand Glu-Chol was reported in our previous report.[15]

4.3. Preparation and characterization of liposomes

Liposomes were prepared by thin film hydration method. Lipid compositions of the prepared liposomes were as follows: (1) conventional liposomes (Lip), SPC/cholesterol/ (molar ratio = 62: 33); (2) Ligand Glu-Vc-Chol modified liposomes (Glu-Vc-Lip), SPC/cholesterol/ligand Glu-Vc-Chol (molar ratio = 62: 33: 3); (3) Ligand Glu-Chol modified liposomes (Glu-Lip), SPC/cholesterol/Ligand Glu-Chol (molar ratio = 62: 33: 3); (4) Ligand Vc-Chol modified liposomes (Vc-Lip), SPC/cholesterol/Ligand Vc-Chol (molar ratio = 62: 33: 3); (5) Ligand Glu-Chol and Vc-Chol co-modified liposomes (Glu+Vc-Lip), SPC/cholesterol/Ligand Glu-Chol/Vc-Chol (molar ratio = 62: 33: 3: 3). All lipid materials were dissolved in the chloroform/methanol (v/v = 2:1), and then the organic solvent was removed by rotary evaporation to get a lipid film, which was further dried in vacuum overnight. Next, the film was hydrated in PBS (pH 7.4) for 0.5 h at 20 ^{o}C. Finally, it was further sonicated intermittently by a probe sonicator at 80 W for 80 s to form liposomes. PTX-loaded liposomes were prepared with paclitaxel added to the lipid organic solution prior to the solvent evaporation. The entrapment efficiency of paclitaxel was determined by HPLC. Likewise, CFPE-labelled liposomes were prepared by adding appropriate amount of CFPE to the solution before removing the solvent. The mean size and zeta potential of Lip, Glu-Vc-Lip, Glu-Lip, Vc-Lip and Glu+Vc-Lip were detected by Malvern Zeta sizer Nano ZS90 (Malvern Instruments Ltd., UK).

4.4. In vitro drug release study

In vitro paclitaxel release study was performed using dialysis method. PTX-loaded liposomes (0.4 mL) or naked paclitaxel were added into dialysis tubes (MWCO = 8000 - 14000 Da) respectively and sealed tightly. Then the dialysis tubes were placed into 40 ml PBS containing 0.1% (v/v) Tween 80 and incubated under 37 °C for 48 h with gentle oscillating at 45 rpm. At predetermined time points (0 h, 1 h, 2 h, 4 h, 8 h,

12 h, 24 h and 48 h), 0.1 ml release medium was taken out and replaced with equal volume of fresh release medium. Then the samples were diluted with acetonitrile and the concentrations of paclitaxel were determined at the wavelength of 225 nm by HPLC.

4.5. In vitro stability of liposomes in serum

The serum stability of liposomes was evaluate by measuring the turbidity variations in the presence of fetal bovine serum (FBS). Briefly, each liposome was mixed with FBS (v/v=1:1) under 37 °C with moderate shaking at 45 rpm. The transmittance of the mixture was measured at predetermined time points (0 h, 1 h, 2 h, 4 h, 8 h, 12 h, 24 h and 48 h) by a microplate reader at 750 nm (Thermo Scientific Varioskan Flash, USA).

4.6. Hemolysis assays

The safety of ligands-modified liposomes during body circulation was demonstrated by hemolysis assay. Fresh mouse blood was collected in tubes containing heparin sodium. The red blood cells (RBCs) were separated and collected by centrifugation at 5×10^3 rpm for 5 min and washed several times with PBS until the supernatant became colorless. After the last wash, the RBCs were diluted with PBS to the concentration of 2% (v/v). The RBCs solutions were incubated with various concentrations of liposomes (v/v=1:1) for 1 h at 37 °C with gentle shaking, followed by centrifugation at 1×10^4 rpm for 10 min. Absorbance of hemoglobin was measured using a microplate reader at 540 nm. The values for 0% and 100% hemolysis were determined by incubating erythrocytes with PBS or 1% (v/v) Triton X-100. The hemolysis percentage was calculated using the following equation:

$$\text{The percent hemolysis} = \frac{A_{Sample} - A_{Negative}}{A_{Postive} - A_{Negative}} \times 100\%$$

where A is the ultraviolet absorbance of hemoglobin.

4.7. Cytotoxicity

The cytotoxicity of PTX-loaded liposomes and blank liposomes against C6 cells ($GLUT_1$ and $SVCT_2$-positive) was measured with MTT assay. Generally, the cells were seeded in a 96-well plate at a density of 5×10^3 cells/well and cultured for 24 h at 37 ^oC. PTX-loaded liposomes and free paclitaxel were diluted to 0.016, 0.08, 0.4, 2, 10, 50 μg/ml of PTX with medium, followed by being added into each well and incubated for 24 h. What's more, the blank liposomes were added at the same concentration of PTX-loaded liposomes. Then, remove the medium and add 200 μl medium containing MTT solution (0.5 mg/ml) to each well. After incubation for another 4 h at 37 °C, the medium was removed and the reduced MTT dye was solubilized by DMSO (150 μl). The optical density (OD) value was read at 490 nm on an automatic microplate spectrophotometer. Cell viability (%) was calculated as the following equation: OD_{test} / $OD_{control}$ × 100%.

4.8. Cellular uptake study

C6 cells were seeded in 12-well plates at a density of 5×10^5 cells/well and cultured for 24 h at 37 ^oC to reach 80% confluence. Different CFPE-labeled liposomes were added into each well with the final concentration of CFPE at 2 μg/ml. After cultured for 4 h at 37 ^oC, the cells were washed with cold PBS. and trypsin was used to harvest the cells afterward. Then, the cells were washed with cold PBS and finally resuspended in 0.5 ml PBS to measure the fluorescent intensity by a flow cytometer at Ex 495 nm and Em 515 nm (BD FACS celestra).

For confocal microscope studies, C6 cells were plated onto a 6-well plate containing cover glass at a density of 5×10^5 cells/well and cultured for 24 h at 37 ^oC. CFPE-labeled liposomes were added into each well and further co-incubation for 4 h. Following that, the cells were fixed with 4% paraformaldehyde for 30 min at room temperature after rinsed with cold PBS for three times, and then cell nuclei were stained with DAPI (5 μg/ml) for 5 min. Finally, the samples were imaged using CLSM (LSM 800, ZEISS,

German). What's more, the intracellular localization of liposomes was also studied. After co-incubation with CFPE-labeled liposomes for 1 h or 4 h, the cells were washed with cold PBS and treated with Lyso-Tracker RED (50 nM, Solarbio) for 1 h at 37 ^{o}C. And then, the cells were fixed and the cell nuclei were stained. Finally, the samples were imaged using CLSM.

In order to research the uptake mechanism of Glu-Vc-Lip, C6 cells were preincubated with various endocytosis inhibitors, such as chlorpromazine (20 μg/ml), sucrose (137 mg/ml), β-cyclodextrin (5.68 mg/ml) and amiloride (1.48 mg/ml). What's more, the inhibition of free glucose (5 mg/ml) and free Vc (88 mg/ml), and the effect of temperature were also performed. Briefly, the cells were preincubated with different inhibitors for 30 min, then the inhibitors were withdrawn from the wells and CFPE-labeled Glu-Vc-Lip was added. After cultured for 4 h at 37 ^{o}C, the cells were treated as described before and the fluorescent intensity was measured by a flow cytometer.

4.9. Distribution in brain and pharmacokinetic studies in mice

4.9.1 Sample preparation

Blood was collected from the eye socket of mouse, and centrifuged at 5000 rpm for 5 min to get the supernatant as plasma sample. Then the animals were sacrificed to get the brains and flushed with saline to remove the remained blood and the main vessel. All the brain tissues were homogenized with saline (w/w=1:3). An aliquot of 10 μl of internal standard (docetaxel, 30 μl, 100 μg/ml) was added into 100 μl plasma or 100 μl brain homogenate, and extracted with 200 μl ether. The mixture was vortexed for 5 min, and centrifuged at 10000 rpm for 10 min. The supernatant was dried and the residue was reconstituted with 100 μl methanol. The solution was centrifuged at 10000 rpm for 10 min, and then 20 μl of the supernatant was injected into the HPLC system for analysis.

4.9.2 Body distribution study

The mice were divided into five groups for each liposome or paclitaxel randomly. PTX-Lip, PTX-Glu-Lip, PTX-Vc-Lip, PTX-Glu-Vc-Lip, PTX-Glu+Vc-Lip and paclitaxel were given to the mice via the tail vein at the dose of paclitaxel of 10 mg/kg. At 5 min, 15 min, 30 min, 60 min, 120 min, 240 min, 480 min and 1440 min after injection, the blood the brain samples were prepared described earlier. The concentration of paclitaxel was analyzed by HPLC.

4.9.3 Statistical analysis

The area under the concentration-time profile (AUC_{0-t}), maximal concentration (C_{max}), and mean residence times (MRT) were calculated by Data and max Statistics (DAS 2.0, Shanghai, China). Statistical evaluation was performed using analysis of variance followed by t-test. A value of $p < 0.05$ was considered significant. The relative uptake efficiency (Re) and concentration efficiency (Ce) were calculated to evaluate the brain targeting property of liposome. The value of Re and Ce were defined as follows:

$Re = (AUC_{0-t})_L / (AUC_{0-t})_P$

$Ce = (C_{max})_L / (C_{max})_P$,

where L and P represented the liposomes loading PTX and paclitaxel, respectively.

4.10. In vivo imaging

Kunming mice (male) were anesthetized with 4% chloral hydrate and placed on a stereotaxic apparatus. 5 μl of C6 cells (2×10^8 cells/mL) were injected into the striatum (1.8 mm lateral, 0.6 mm anterior to the bregma and 3 mm of depth) of each mouse. After 14 days, the mice were randomly divided into 5 groups and were intravenously injected via the caudal vein of the tumor-bearing mice with DiD loaded different liposomes DiD-Lip, DiD-Glu-Lip, DiD-Vc-Lip, DiD-Glu-Vc-Lip and DiD-Glu+Vc-Lip at a dose of 200 μg/kg. Then, the mice were anesthetized with 4% chloral hydrate and imaged with IVIS Lumina Series III imaging system (LIVIS Lumina III, Perkin Elmer, USA) at 1 h, 2 h, 6 h and 24 h after injection. The mice

were sacrificed after heart perfusion with saline at these pre-determined time points. Brains, hearts, livers, spleens, lungs and kidneys were collected. All the organs were also imaged with IVIS Lumina Series III imaging system.

Acknowledgement

This work was supported by the National Natural Science Foundation of China (No.81573286, No.81773577, No.21472130 & No.81603218).

References

1. Razpotnik R, Novak N, Serbec VC, et al. Targeting Malignant Brain Tumors with Antibodies. *Front Immunol*. 2017;8:1181.
2. Zhang X, He XX, Chen QH, et al. A review on the hybrids of hydroxycinnamic acid as multi-target-directed ligands against Alzheimer's disease. *Bioorg Med Chem*. 2018;26:543-550.
3. Bruce H, Morimoto. Therapeutic peptides for CNS indications: Progress and challenges. *Bioorg Med Chem*. 2018;26:2859–2862.
4. Barbara R, Belletti D, Pederzoli F, et al. Novel Curcumin loaded nanoparticles engineered for Blood-Brain Barrier crossing and able to disrupt Abeta aggregates. *Int J Pharm*. 2017;526:413-424.
5. Kuo YC, Rajesh R. Targeted delivery of rosmarinic acid across the blood-brain barrier for neuronal rescue using polyacrylamide-chitosan-poly(lactide-co-glycolide) nanoparticles with surface cross-reacting material 197 and apolipoprotein E. *Int J Pharm*. 2017;528:228-241.
6. Zhao GJ, Huang Q, Wang F, et al. Targeted shRNA-loaded liposome complex combined with focused ultrasound for blood brain barrier disruption and suppressing glioma growth. *Cancer Lett*.

2018;418:147-158.

7. Zhao Y, Qu BY, Wu XY, et al. Design, synthesis and biological evaluation of brain targeting L-ascorbic acid prodrugs of ibuprofen with "lock-in" function. *Eur J Med Chem*. 2014;82:314-323.
8. Alex AT, Joseph A, Shavi G, et al. Development and evaluation of carboplatin-loaded PCL nanoparticles for intranasal delivery. *Drug Deliv*. 2016;23:2144-2153.
9. Ghasemy S, Garcia-Pindado J, Aboutalebi F, Fine-tuning the physicochemical properties of peptide-based blood-brain barrier shuttles. *Bioorg Med Chem*. 2018;26:2099-2106.
10. Yang XL, Cai P, Liu QH, et al. Novel 8-hydroxyquinoline derivatives targeting b-amyloid aggregation, metal chelation and oxidative stress against Alzheimer's disease. *Bioorg Med Chem*. 2018;26:3191–3201.
11. Yue QM, Peng Y, Zhao Y, et al. Dual-targeting for brain-specific drug delivery: synthesis and biological evaluation. *Drug Deliv*. 2018;25:426-434.
12. Zhao Y, Zhang L, Peng Y, et al. GLUT1-mediated venlafaxine-thiamine disulfide system-glucose conjugates with "lock-in" function for central nervous system delivery. *Chem Biol Drug Des*. 2018;91:707-716.
13. Qu BY, Li X, Wu JB, et al. Synthesis of Multivalent Glucosides with High Affinity for GLUT1 Transporter. *Lett Org Chem*. 2012;9:390-395.
14. Xie FL, Yao N, Qin Y, et al. Investigation of glucose-modified liposomes using polyethylene glycols with different chain lengths as the linkers for brain targeting. *Int J Nanomed*. 2012;7:163-175.
15. Samaridou E, Alonso MJ. Nose-to-brain peptide delivery-The potential of nanotechnology. *Bioorg Med Chem*. 2018;26:2888–2905.
16. Qu BY, Li XC, Guan M, et al. Design, synthesis and biological evaluation of multivalent glucosides

with high affinity as ligands for brain targeting liposomes. *Eur J Med Chem*. 2014;72:110-118.

17. Subbaiah MAM, Meanwell NA, Kadow JF. Design strategies in the prodrugs of HIV-1 protease inhibitors to improve the pharmaceutical properties. *Eur J Med Chem*. 2017;139:865-883.
18. Fan W, Wu Y, Li XK, et al. Design, synthesis and biological evaluation of brain-specific glucosyl thiamine disulfide prodrugs of naproxen. *Eur J Med Chem*. 2011;46:3651-3661.
19. Li XC, Qu BY, Jin XX, et al. Design, synthesis and biological evaluation for docetaxel- loaded brain targeting liposome with "lock-in" function. *J Drug Target*. 2014;22:251-261.
20. Wang LH, Zhao Y, Lu RX, et al. Preparation and Characterization of Novel Brain Targeting Magnetic Nanoparticles Modified with Ascorbic Acid. *NANO*. 2018;13:1850008
21. Kato E, Kimura S, Kawabata J. Ability of higenamine and related compounds to enhance glucose uptake in L6 cells. *Bioorg Med C hem.* 2017;25:6412–6416.
22. Chen Q, Gong T, Liu J, et al. Synthesis, in vitro and in vivo characterization of glycosyl derivatives of ibuprofen as novel prodrugs for brain drug delivery. *J Drug Target*. 2009;17:318-328.
23. Chu KF, Yao CH, Song JS, et al. N-Indolylglycosides bearing modifications at the glucose C6-position as sodium-dependent glucose co-transporter 2 inhibitors. *Bioorg Med Chem.* 2016;24:2242–2250.
24. da Silva AX, Lavialle F, Gendrot G, et al. Glucose transport and utilization are altered in the brain of rats deficient in n-3 polyunsaturated fatty acids. *J Neurochem*. 2002;81:1328-1337.
25. Corpe CP, Lee JH, Kwon O, et al. 6-bromo-6-deoxy-L-ascorbic acid - An ascorbate analog specific for Na^+-dependent vitamin C transporter but not glucose transporter pathways. *J Biol Chem*. 2005;280:5211-5220.